Discussion

Shearless bifurcation on symplectic maps of magnetic field lines in tokamaks with reversed current

B. Bartoloni [a],*, A.B. Schelin [b], I.L. Caldas [c]

[a] *Instituto de Física, Universidade de São Paulo, Rua do Matão, 1371, 05508-090, São Paulo, SP, Brazil*
[b] *Instituto de Física, Universidade de Brasília, Campus Universitário Darcy Ribeiro, 70910-900, Brasília, Distrito Federal, Brazil*
[c] *Instituto de Física, Universidade de Brasília, Rua do Matão, 1371, 05508-090, São Paulo, SP, Brazil*

A B S T R A C T

We introduce two-dimensional symplectic maps to describe the Poincaré maps of magnetic field lines in large aspect ratio tokamak equilibria with reversed non-monotonic plasma current density profiles. For these maps, we investigate the effect of the symmetry breaking due to the toroidal correction with a peculiar invariant, namely, a magnetic surface with a null rotation number, enclosing a vanishing current. We find that this rotationless invariant surface is surrounded by many small island chains. Furthermore, near such invariant, the symmetry breaking gives rise to two magnetic shearless invariants surrounded by twin island chains. We also find chaotic lines adjacent to all the observed islands created by the considered structurally unstable equilibria.

© 2016 Elsevier B.V. All rights reserved.

1. Introduction

Two-dimensional symplectic maps have been introduced to describe Poincaré maps of magnetic field lines in confined plasmas. In fact, magnetic field lines can be described by orbits of Hamiltonian systems of one-and-a-half degrees of freedom which are, provided the time-like coordinate is periodic, equivalent to two-dimensional area-preserving maps [1–4]. Consequently, we can use such maps to describe field lines in magnetic configurations of plasmas confined in tokamaks, and to interpret plasma confinement properties in the nonlinear dynamics framework. The considered magnetic configurations are essentially a superposition of two magnetic field components: toroidal, which is produced by coils around the chamber, and poloidal, which is produced by plasma current. Thus, the magnetic field lines are helices on nested toroidal magnetic surfaces characterized by their rotation number [5]. These toroidal surfaces are invariants identified as lines in the associated Poincaré maps.

Several symplectic maps [6] have been introduced to describe the field lines dynamics in tokamaks. Two of them, the Ullmann map [7,8] and the Tokamap [9], introduced to describe large aspect ratio tokamaks with toroidal correction, have been applied to analyze field line dynamics of confined plasmas with field lines

with monotonic or nonmonotonic rotation number profiles [2]. The form of the rotation number profile is essentially determined by the electrical current density profile inside the confined plasma. The Ullmann map is more convenient to compare with experimental results because we can introduce in the map expressions the experimental equilibrium profiles, as the plasma current density. Although the tokamap parameters do not correspond to tokamak experimental values, this map is appropriate to investigate general dynamical effects in tokamaks as the onset of global chaos and bifurcations.

In this article, we investigate the dynamics of plasmas with a reversed density current profile (negative density current at plasma center), which leads to a magnetic field with nonmonotonic rotation number profiles vanishing in a magnetic surface. Evidences of such reversed current profiles have already been observed in tokamaks experiments [10–12]. Likewise, considering reversed density currents, analytical and numerical works have also reported instability predictions [13,14], as well as magnetohydrodynamic equilibrium solutions with non-nested magnetic surfaces [15–19]. All the reported equilibria, obtained for small inverse aspect ratio toroidal tokamaks (ratio between the minor and major tokamak radii), describe KAM invariant curves in the Poincaré maps, with one island chain in the null rotation region, without chaos.

We apply the symplectic Ullmann map and the Tokamap mentioned before to study the field lines Poincaré sections of magnetic fields in plasmas with reversed current density, in large aspect ra-

* Corresponding author. Tel.: +55 1130916842, +55 1142293855.
E-mail addresses: bartolonis@yahoo.com.br (B. Bartoloni), aschelin@gmail.com (A.B. Schelin), ibere@if.usp.br (I.L. Caldas).
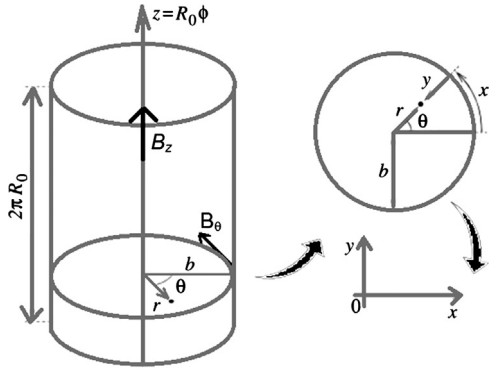
Fig. 1. Tokamak scheme showing the main coordinate systems and the cylindrical approximation. Also we represent the poloidal and toroidal magnetic fields.

tio tokamaks with toroidal correction [8]. In our procedure, the small correction parameter is the inverse of the aspect ratio. We investigate the effect of the symmetry breaking due to the toroidal correction in these maps with a peculiar invariant, a null rotation number, representing a magnetic surface enclosing a vanishing current. We find that this rotationless invariant surface is surrounded by many small island chains and localized chaotic field lines around these islands. Furthermore, near such invariant, the symmetry breaking gives rise to two magnetic shearless invariants surrounded by twin island chains. Thus, the main result in the article is not only the appearance of small islands and chaos, but also the unexpected onset of shearless invariant curves in the maps due to the symmetry break caused by the toroidal correction.

In Section 2 we introduce the symplectic two-dimensional Ullmann map for a reversed current profile. In Section 3 we present evidences of shearless bifurcations due to the symmetry breaking by the toroidal correction. Section 4 contains map amplifications with small islands surrounded by chaotic lines. In Section 5 we present similar results obtained for the Tokamap, another symplectic two-dimensional map known in literature. Finally, the conclusions are discussed in Section 6.

2. Ullmann map

In tokamaks, magnetic fields are established for the plasma confinement in a toroidal chamber. The plasma is mainly confined by the superposition of two magnetic field components: toroidal, which is produced by coils around the chamber, and poloidal, which is produced by plasma current [4,5]. In this work we consider a reversed density current profile, with negative density current at plasma center as, recently, observed in tokamaks [10–12].

The tokamak geometry is shown in Fig. 1. The toroidal vessel is characterized by its major radius R_0, which defines the circular geometric axis around the axis of the toroid, and by its minor radius b. Usually we define the aspect ratio in a tokamak as $\varepsilon = R_0/b$. The coordinates r and θ are, respectively, the radius from the geometric axis and the poloidal angle, and $\emptyset$ is the toroidal angle. We consider a tokamak with large aspect ratio (high ε), and, for such approximation, the equilibrium toroidal magnetic field is approximately uniform and therefore the effect of the toroidal curvature can be considered as a perturbative factor [2,8]. Thus, we can adopt a cylindrical geometry, with period $2\pi R_0$, as shown in Fig. 1. The rectangular coordinates system, suitable to describe our problem, is given by equations $x = b\theta/2\pi$, $y = 1 - r/b$, and $z = R_0\emptyset$, where b and R_0 are, respectively, the minor and the major tokamak radii. In this coordinate system, $y = 0$ corresponds to the plasma edge and $y = 1$ corresponds to the plasma center. In the next sections, for the numerical applications, we use the main TCABR tokamak parameters, as $b = 0.21$ m and $R_0 = 0.61$ m [20].

The magnetic field lines resulting from the sum of the poloidal and toroidal components have a helical format. The toroidal field line component is uniform, $B_z \equiv B_0$, and, given a current density radial profile, $J_z(r)$, the poloidal magnetic field component, B_θ, is obtained from the Ampère's Law. The field helicity is given by the average rotation number ι, whose inverse is known as the safety factor in the tokamak literature [2,8], defined as:

$$q_0 = 1/\iota \quad \Rightarrow \quad q_0 = \frac{1}{2\pi} \int_0^{2\pi} \frac{B_z}{B_\theta} d\theta \tag{1}$$

Thus, for each poloidal magnetic field profile we have a correspondent rotation number profile.

The structure of the magnetic field lines in a tokamak can be more easily studied by means of a return map – whose trajectories are obtained from the continuous trajectories arbitrating a region in the phase space and taking the coordinate values only at the intersection with the surface. A return map in $\emptyset$ coordinate consists in a Poincaré map in the section $z = constant$, with variables (r_n, θ_n) or (x_n, y_n) denoting the coordinates on the section surface (the coordinates of the nth intersection of the field line with the surface provides the following position) [2,4,5].

Our map consists of two equations:

$$r_{n+1} = \frac{r_n}{1 - a_1 sen\theta_n} \tag{2}$$

$$\theta_{n+1} = \theta_n + \frac{2\pi}{q(r_{n+1})} + a_1 \cos\theta_n \tag{3}$$

where $a_1 = -0.04$ is a correction due to the toroidal effect and $q(r)$ is the safety factor profile [7]. The toroidal correction introduces a poloidal angle θ dependence in the map. Such correction, considered in the model, takes into account the outward magnetic surfaces displacement, characteristic of tokamak equilibrium in the toroidal geometry. The constant $a_1 = -0.04$ was fitted to reproduce the observed tokamak magnetic surfaces displacements [7]. The Jacobian for this map is unitary, so the map is symplectic [4,6]. Moreover, the map is derived from a generating function and can be interpreted as a canonical transformation between the previous and the next coordinates.

The map given by equations (2) and (3) is determined by the control parameters and the function $q(r)$ is specified for the desired plasma equilibrium, i.e., obtained from the considered magnetic field components B_z and B_θ. Thus, we have to introduce a plasma current density, $J_z(r)$, to obtain the magnetic component B_θ.

In this article, we consider a non-monotonic current density profile J_z, with a reversed current

$$J_z(r) = \frac{I_p R_0}{\pi a^2} \frac{(\delta + 2)(\delta + 1)}{\delta + \gamma + 2} \left(1 + \delta \frac{r^2}{a^2}\right) \left(1 - \frac{r^2}{a^2}\right)^\gamma \tag{4}$$

where $a = 0.18$ m is the plasma radius, $I_p = 20$ kA is the plasma current. We also have the parameters $\delta = -100.2$ and $\gamma = 5$ [18]. All these parameters are from TCABR tokamak [20]. For negative values of δ, the poloidal field has negative and positive values, changing signal at the divergence surface. For positive values the poloidal field is positive everywhere. The parameter γ increases with the field line shear at the plasma edge. From Equation (4), we determine the radial position for which the current density changes signal, namely $r_c = a/\sqrt{-\delta}$.

This reversed current profile is shown in Fig. 2, where $y = 0$ corresponds to the plasma edge and $y = 1$ corresponds to the plasma center. Recently, other theoretical works have considered similar reversed density magnetohydrodynamic equilibrium solutions, analytical and numerical, with non-nested magnetic surfaces [15–19].
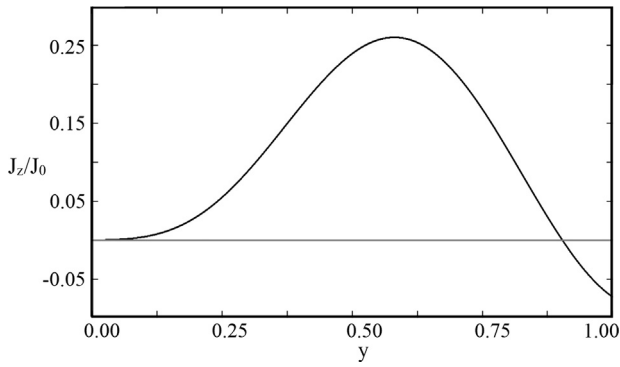
Fig. 2. Reversed current density profile. We have a central region where the current density becomes negative ($y = 0$ at the plasma edge and $y = 1$ at the center).

For the considered J_z, we calculate the magnetic field by Ampère's Law. In Fig. 3(a), we reproduce the poloidal field profile and the equilibrium safety factor profile, which is given by:

$$q_0(r) = q(a) \frac{r^2}{a^2} \left[1 - \left[\left(1 + \beta' \frac{r^2}{a^2} \right) \left(1 - \frac{r^2}{a^2} \right)^{\gamma+1} \right]^{-1} \right]$$

$$\times \left[1 - 4 \left(\frac{r}{R_0} \right)^2 \right]^{-1/2} \quad (5)$$

where $q(a) = \varepsilon a^2 / R_0^2 = 5.0$ and $\beta' = \delta(\gamma + 1)/(\delta + \gamma + 2)$ with $\delta = -100.2$ and $\gamma = 5$.

The equilibrium safety factor profile of Fig. 3(a) has a divergence at the radial position where the poloidal magnetic field is zero and, consequently, the magnetic surface encloses a null current density. Such divergence corresponds to a null rotation number and originates the peculiar effects analyzed in the next sections.

In the large aspect ratio equilibrium, $\varepsilon \sim \infty$ and $a_1 = 0$, the map gives invariants with constant y. In the invariant horizontal lines the orbits are quasi periodic (periodic) if q is irrational (rational). Each invariant line has a rotation number obtained from equation (5), and one of theses invariants has a null rotation number.

3. Shearless bifurcations

Next we analyze the alterations in the Poincaré map due to the toroidal correction (finite ε) introduced by considering the parameter $a_1 = -0.04$ in equations (2).

The field component in Fig. 3(a) is null in the region where $y = 0.876$. This null component causes a divergence in the expression for $q_0(y)$ in this position, as it can be seen in Fig. 3(b). This safety factor was obtained taking into account the equilibrium symmetry, namely, its independence of coordinate θ. However, the toroidal correction introduces a dependence on θ and a ripple in the modified invariant curves. Thus, the modified safety factor has to be calculated numerically, from the average rotation number, according to the definition:

$$q \equiv \lim_{k \to \infty} \frac{2\pi k}{\sum_{j=0}^{k} (\theta_{j+1} - \theta_j)} \quad (6)$$

Fig. 4(a) shows the modified profile $q(y)$, obtained by fixing $x = 0.510$ and calculating numerically the safety factor for 100 values of y between 0 and 1.

Fig. 4(a) shows a divergence (null rotation number) at $y = 0.916$ (it is not in $y = 0.876$, as in Fig. 3(b), because here we take
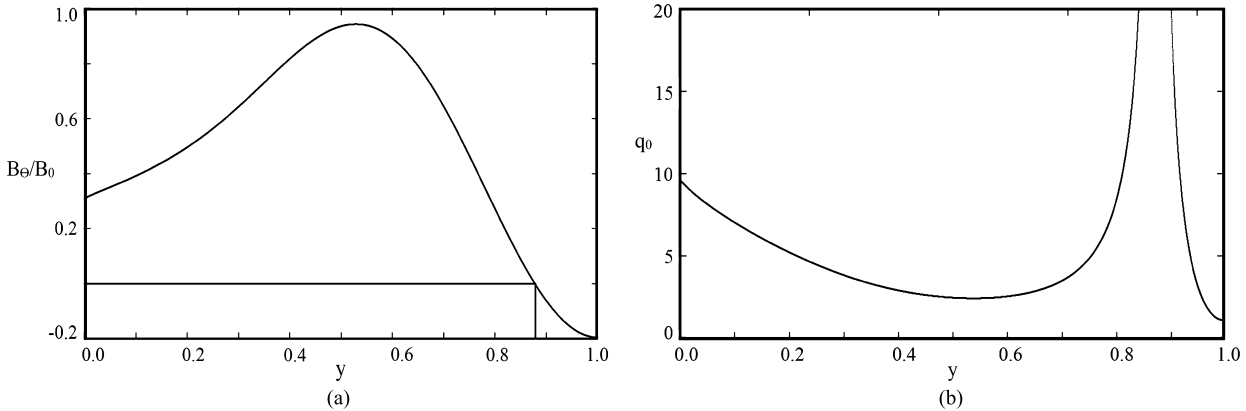

Fig. 3. (a) Poloidal magnetic field profile, which is null at $y = 0.876$; (b) Safety factor profile, with a divergence in $y = 0.876$.
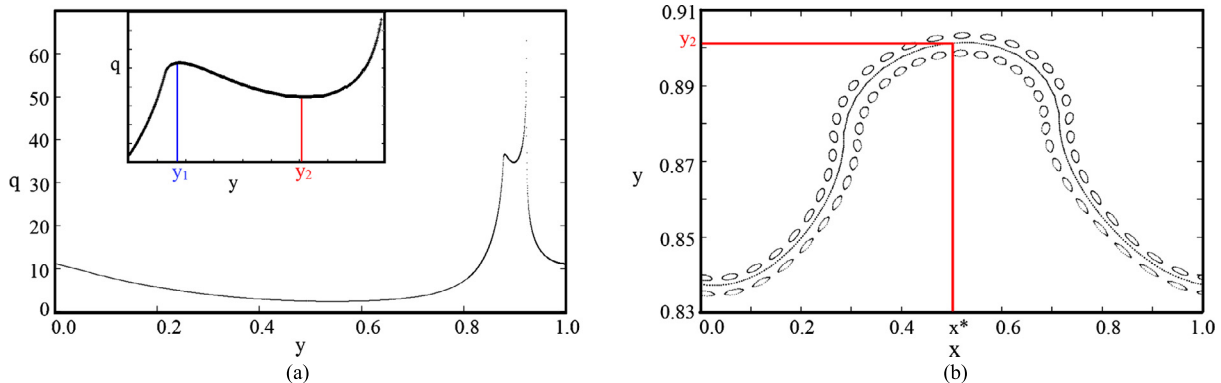

Fig. 4. (a) Numerical safety factor profile. We fixed $x = 0.51$ to obtain this profile. In the inset, we highlight the maximum and minimum points; (b) Shearless line and island chains.
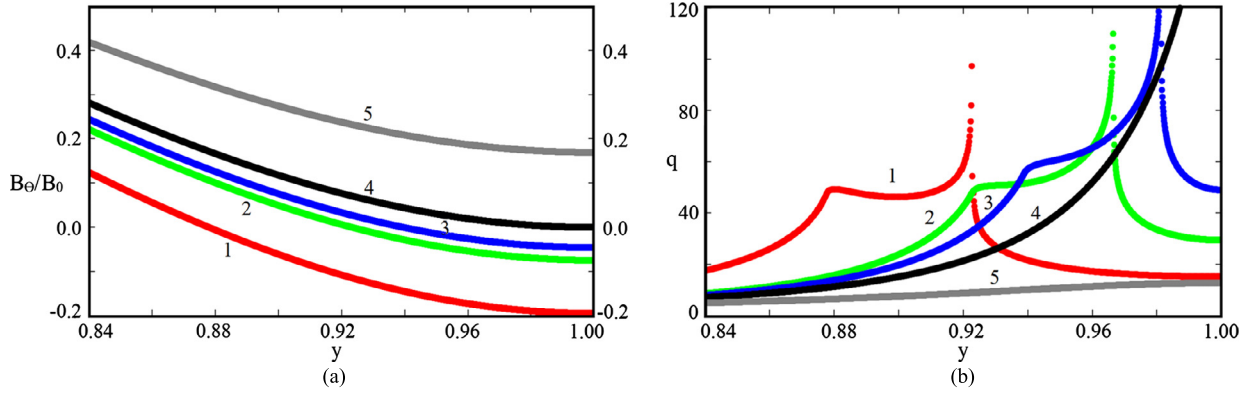
Fig. 5. (a) Magnetic field profiles for various values of δ in reversed current region. Reversed current region (negative magnetic field) becomes smaller with the increase, in modulus, of δ. (b) Numerical safety factor profile for same values of δ. Values of δ: -100.2 (curve 1), -250.2 (curve 2), -400.2 (curve 3), -46000.2 (curve 4) and 100.2 (curve 5).

into account the toroidal correction). Therefore, $y = 0.916$ is the position of the surface with a null rotation number displaced by the toroidal correction.

In Fig. 4(a) we see two points where $\partial q / \partial y = 0$ (in $y = 0.903$ and $y = 0.873$), i.e., these two points are in shearless invariant curves [4,6]. Around each of these shearless curves we expect to observe twin island chains with the same rotation number, as it is shown in Fig. 4(b) for one of the indicated shearless lines.

To investigate the onset of the shearless bifurcations we vary the values of δ in the expression for J_z (equation (4)), for the same plasma current $I_p = 20$ kA.

Fig. 5(a) presents the equilibrium poloidal field radial profiles for five values of δ chosen to show the influence of the reversed current region, with negative poloidal field, on the shearless bifurcation. To verify this influence, we present in Fig. 5(b) the modified safety factor profiles corresponding to the field profiles of Fig. 5(a).

We notice in Fig. 5(a) that, for curves 1, 2, 3, the region in which we have the reversed current (negative magnetic field) becomes smaller with the increase, in modulus, of δ. Curve 4 corresponds to $\delta = -46000.2$ and we can see that the field is positive and ends at zero for $y = 1$, i.e., the current density profile becomes only non-monotonic, without reversed current. In Fig. 5(b) we reproduce the modified safety factor profiles for the same values of δ and we can see that the distance between the critical points also decreases until they disappear in the curve 4 (again it corresponds to $\delta = -46000.2$). For this critical δ value, we do not have island chains in Poincaré sections. Therefore, we can conclude that the appearance of chain islands is directly related to δ parameter.

The same effect is observed whenever we vary the toroidal correction parameter a_1. As we decrease the value of a_1, in modulus, we also realize that the distance between the critical points decreases until they disappear in the limit of a_1 going to zero, as we see in Fig. 6 (we fixed the parameter $\delta = -100.2$).

4. Island and chaos

In Fig. 7(a) we have a Poincaré section of Ulmann map. The blue line indicates the divergence curve. The rectangle indicates the region to which we have a zoom, in Fig. 7(b).

We can see that, unexpectedly, the Poincaré section given by the map without perturbation, close to divergence curve, has many small islands (Fig. 7(a)) and localized chaos (Fig. 7(b)).

To study this behavior, we calculate again the modified safety factor profile $q(y)$ for initial conditions close to the divergence curve.

In Fig. 8(a), we fixed $x = 0.49$ along the line shown in the Poincaré section in Fig. 7(a). If the value of the numerical safety
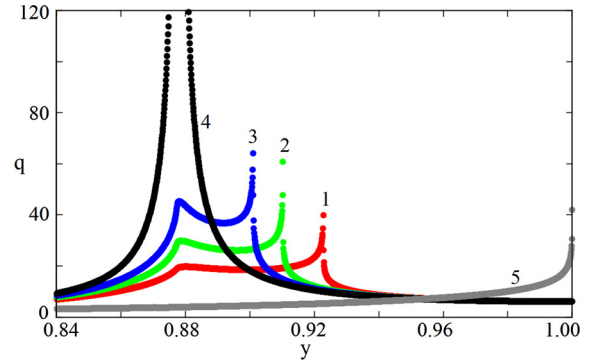

Fig. 6. Numerical safety factor profile for some values of a_1. Values of a_1: -0.04 (curve 1), -0.02 (curve 2), -0.01 (curve 3), 0.00 (curve 4) and 0.30 (curve 5).

factor does not converge, we have a chaotic trajectory. All values converge, see Fig. 8(a), indicating that the chaos is quite located. When we have a chain, the value of the numerical safety factor is constant, and we can observe various levels corresponding to the passages through the island chains. When we make a zoom in Fig. 8(a), we can see the same behavior, with the levels where the numerical safety factor is constant (Fig. 8(b)). This characteristic is known in the literature as *devil's staircase* and can also be observed in a circle map [21]. These many levels show that we have many small islands, as observed in Fig. 7(a).

We see that in the large aspect ratio tokamak approximation, for a reversed current density profile, the toroidal correction introduces many small island chains and an extremely localized chaos.

5. Tokamap

In this section we show that the results described in the previous sections can also be obtained for another two-dimensional symplectic map, the Tokamap, found in the literature to analyze magnetic field line dynamical properties [9].

The Tokamap is a well established Hamiltonian map proposed by Balescu et al. to model magnetic field lines compatible with a toroidal geometry [9,22–26]. The motion of magnetic field lines is described by a Poincaré map where:

$$(\psi_{k+1}, \theta_{k+1}) = \hat{P}(\psi_k, \theta_k) \tag{7}$$

relating the intersection point (ψ, θ) of the field line with the poloidal section $\emptyset = const$ to the next point $(\psi_{n+1}, \theta_{n+1})$ after the toroidal turn. Specifically, the Tokamap is given by the following set of equations:
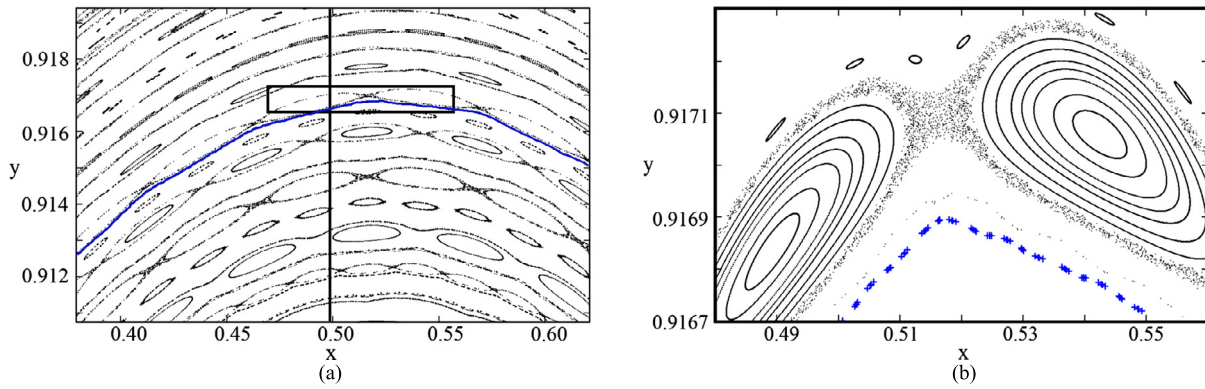
Fig. 7. (a) Poincaré section close to the divergence curve. (b) Amplification of the area indicated by a box in (a), where we can see many small islands and a chaotic field line.
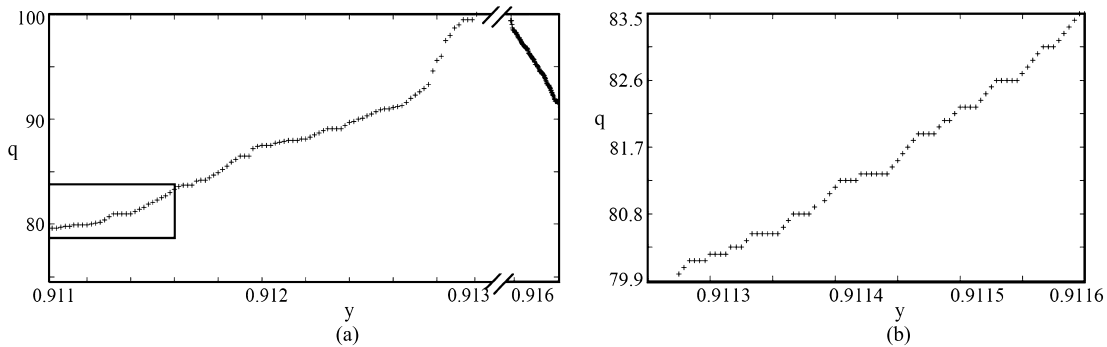

Fig. 8. (a) Numerical safety factor profile. (b) Amplification of the profile box showing the levels when the values are constants, indicating the presence of the islands.

$$\psi_k = \psi_k - \frac{L}{2\pi} \frac{\psi_{k+1}}{1 + \psi_{k+1}} \sin(2\pi\theta_k) \tag{8}$$

$$\theta_{k+1} = \theta_k + \frac{1}{q(\psi_{k+1})} - \frac{L}{2\pi} \frac{1}{(1 + \psi_{k+1})^2} \cos(2\pi\theta_k) \tag{9}$$

where ψ is the toroidal flux, θ is the poloidal angle and L is the stochastic parameter.

The Tokamap meets a minimal requirement in order to follow toroidal geometry: the magnetic axis is impenetrable, with $\psi_0 = 0$ implying that $\psi_n > 0$ for all n, and if $\psi_0 = 0$ then $\psi_n = 0$ for any value of n. Equations (2)–(3) are implicit. However, equation (2) can be explicitly solved by:

$$\psi_{k+1} = \frac{1}{2}\left[\sqrt{P^2(\psi_k, \theta_k) + 4\psi_k} - P(\psi_k, \theta_k)\right] \tag{10}$$

where $P(\psi_k, \theta_k) = 1 - \psi_k + \frac{L}{2\pi}\sin(2\pi\theta_k)$.

In the original version of the map the safety profile $q(\psi)$ is given by:

$$\frac{1}{q} = \frac{1}{4}(2 - \psi_{k+1})(2 - 2\psi_{k+1} + \psi_{k+1}^2) \tag{11}$$

In the present work, we are mainly concerned with the reversed current density, which yields the safety profile introduced in section 2. In what follows, we show the consequences of such safety profile on Poincaré plots of magnetic field lines, we use $y = 1 - \psi$ and $x = \theta$.

In the original Tokamap, the Shafranov shift displaces the magnetic axis for small values of the stochastic parameter ($L \ll 1$); for $L = 0$ the tokamap becomes integrable [9]. As an example, Fig. 9 shows the preserved KAM surfaces and the displaced magnetic axis for $L = 0.05$.

In Fig. 10(a) we show the phase portrait obtained with the new safety profile for $L = 0.05$. The line shows the x values used to calculate the numerical safety factor profile in Fig. 10(b).
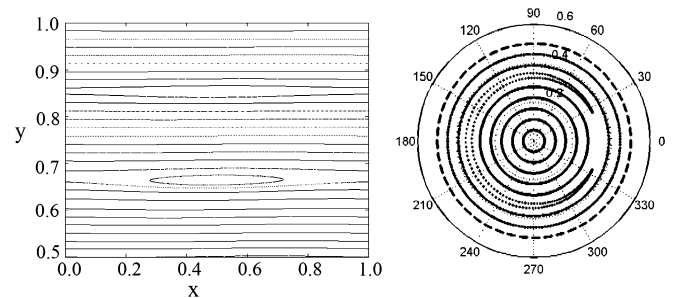

Fig. 9. Regular magnetic surfaces for the original Tokamap with $L = 0.05$.
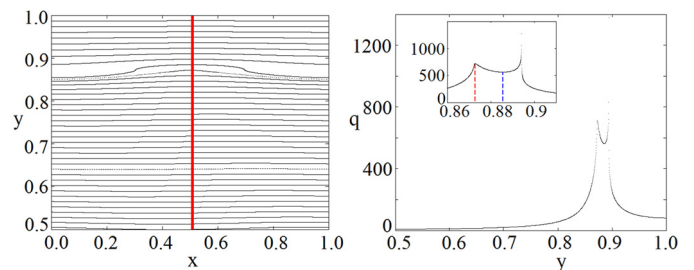

Fig. 10. (a) Phase portrait obtained by the new safety profile for $L = 0.05$. (b) The line shows the $x = 0.51$ used to calculate the numerical safety profile.

As in the previous example, we find two shearless curves ($y_1 = 0.8728$ and $y_2 = 0.8856$) and one divergence ($y = 0.8941$). Around each shearless curve, there are two twin chains of islands, as shown in Fig. 11 for y_2.

Further analysis also shows that even for such small value of L, several small islands and localized chaos appear. Fig. 11 shows an example of such phenomenon.
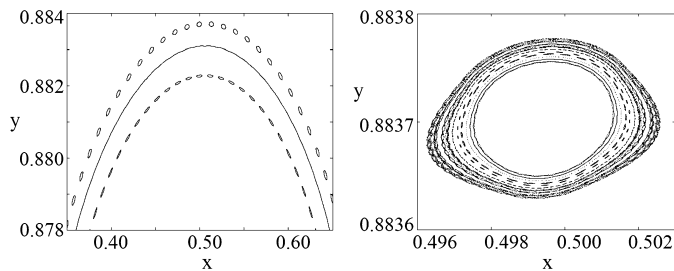
Fig. 11. (a) Chains of magnetic islands. (b) Localized chaos around one island.

Thus, the shearless bifurcations, islands onset and localized chaos found in the Ullmann map are also observed for the Tokamap.

6. Conclusions

We considered two symplectic two-dimensional maps, Ullmann map and Tokamap, with a null rotation invariant surface and a symmetry broken by a small amplitude geometry correction.

These two maps describe magnetic field lines in the limit of large aspect ratio tokamaks, described by plasma cylindrical symmetric equilibria, with a peculiar null rotation invariant two-dimensional surface. A correction taking into account a finite aspect ratio introduces a toroidal field lines curvature around the equilibrium symmetry axis and, consequently, the introduced poloidal dependence on this equilibrium breaking the symmetry, creating islands chains and chaos surrounding the null rotation surface.

Furthermore, with the toroidal correction, two shearless invariant surfaces are created, near the null rotation invariant, in addition to the unperturbed one.

The reported onset of islands, chaos, and shearless invariants in the analyzed maps can be attributed to the breaking of the maps symmetry, due to the small correction introduced to include the field lines toroidal curvature perturbation in the considered structurally unstable equilibria.

Initially, to study the field lines for the tokamak discharges with reversed current density, we applied the Ullmann map which can be related directly to the parameters of a given tokamak and is still symplectic. We splitted our mapping for the Poincaré section immediately following the perturbation in two consecutive ones: the first describing the equilibrium line trajectory along the tokamak chamber and the second describing the effects of the external current coils. Thus, we could investigate the presented effects observed without any external perturbation. Also important was that the toroidal mapping reduced to the cylindrical mapping in the limit of small inverse of the aspect ratio. Furthermore, the map was derived for a generating function, which guarantees its symplecticity [20]. The safety factor profile was chosen to reproduce the considered reversed current density. Moreover, the map allows the introduction of an arbitrary poloidal magnetic field profile and, therefore can be applied for numerical simulations of other future experiments with reversed current density.

Finally, we applied the tokamap to the reversed current density equilibria mainly to validate our results. The obtained confirmation is important because the tokamap have been used in literature to simulate several dynamical properties of field lines in tokamaks. However, to validate our results we had to choose parameters values that could not be directly related to those used in the Ullmann map or measured in tokamak experiments. Our procedure confirmed the reported effects but limits the applicability of tokamap to predict experiments because its parameters do not correspond to experimental values.

Acknowledgements

References

[1] S.S. Abdullaev, Construction of mappings for Hamiltonian systems and their applications, Lect. Notes Phys. 691 (2006) 219–254.

[2] J.S.E. Portela, I.L. Caldas, R.L. Viana, Tokamak magnetic field lines described by simple maps, Eur. Phys. J. Spec. Top. 165 (2008) 195–210, http://dx.doi.org/10.1140/epjst/e2008-00863-y.

[3] A.H. Boozer, Physics of magnetically confined plasmas, Rev. Mod. Phys. 76 (2005) 1071.

[4] P.J. Morrison, Magnetic field lines, Hamiltonian dynamics, and nontwist systems, Phys. Plasmas 7 (2000) 2279, http://dx.doi.org/10.1063/1.874062.

[5] D.R. Hazeltine, J.D. Meiss, Plasma Confinement, Dover Books on Physics, 2003.

[6] J.D. Meiss, Symplectic maps, variational principles, and transport, Rev. Mod. Phys. 64 (1992) 795.

[7] K. Ulmann, I.L. Caldas, A symplectic mapping for the ergodic magnetic limiter and its dynamical analysis, Chaos Solitons Fractals 11 (2000) 2129.

[8] C. Vieira Abud, I.L. Caldas, Onset of shearless magnetic surfaces in tokamaks, Nucl. Fusion 54 (2014) 64010, http://dx.doi.org/10.1088/0029-5515/54/6/064010.

[9] R. Balescu, M. Vlad, F. Spineanu, Tokamap: a Hamiltonian twist map for magnetic field lines in a toroidal geometry, Phys. Rev. E 58 (1998) 951.

[10] T. Fujita, T. Suzuki, T. Oikawa, A. Isayama, T. Hatae, O. Naito, et al., Current clamp at zero level in JT-60U current hole plas, Phys. Rev. Lett. 95 (2005) 075001.

[11] B.C. Stratton, J.A. Breslau, R.V. Budny, S.C. Jardin, W. Park, H.R. Strauss, et al., The role of axisymmetric reconnection events in JET discharges with extreme shear reversal, Plasma Phys. Control. Fusion 44 (2002) 1127.

[12] N.C. Hawkes, B.C. Stratton, T. Tala, C.D. Challis, G. Conway, R. DeAngelis, et al., Observation of zero current density in the core of JET discharges with lower hybrid heating and current drive, Phys. Rev. Lett. 87 (2001) 115001.

[13] G.T. Huysmans, T.C. Hender, N.C. Hawkes, X. Litaudon, MHD stability of advanced tokamak scenarios with reversed central current: an explanation of the "current hole", Phys. Rev. Lett. 87 (2001) 245002, http://dx.doi.org/10.1103/PhysRevLett.87.245004.

[14] J.M. Greene, J.L. Johnson, K.E. Weimer, Tokamak equilibrium, Phys. Fluids 14 (1971) 671.

[15] A.A. Martynov, S.Y. Medvedev, L. Villard, Tokamak equilibria with reversed current density, Phys. Rev. Lett. 91 (2003) 085004.

[16] S. Wang, Theory of tokamak equilibria with central current density reversal, Phys. Rev. Lett. 93 (2004) 155007.

[17] P. Rodrigues, J.P. Bizarro, Grad–Shafranov equilibria with negative core toroidal current in tokamak plasmas, Phys. Rev. Lett. 95 (2005) 015001.

[18] C.G.L. Martins, M. Roberto, I.L. Caldas, F.L. Braga, Analytical solutions for Tokamak equilibria with reversed toroidal current, Phys. Plasmas 18 (2011) 082508, http://dx.doi.org/10.1063/1.3624551, pp. 1–8.

[19] D. Ciro, I.L. Caldas, Magnetic topology and current channels in plasmas with toroidal current density inversions, Phys. Plasmas 20 (2013) 102512, http://dx.doi.org/10.1063/1.4825241.

[20] T. Kroetz, M. Roberto, E.C. da Silva, I.L. Caldas, R.L. Viana, Escape patterns of chaotic magnetic field lines in a tokamak with reversed magnetic shear and an ergodic limiter, Phys. Plasmas 15 (2008) 092310.

[21] R.E. Ecke, J.D. Farmer, D.K. Umberger, Scaling of the Arnold tongues, Nonlinearity 2 (1989) 175–196.

[22] A.B. Schelin, I.L. Caldas, R.L. Viana, S. Benkadda, Collisional effects in the tokamap, Phys. Lett. A, Gen. At. Solid State Phys. 376 (2011) 24–30, http://dx.doi.org/10.1016/j.physleta.2011.10.025.

[23] S.S. Abdullaev, On mapping models of field lines in a stochastic magnetic field, Nucl. Fusion 44 (2004) 6.

[24] J.H. Misguich, J.-D. Reuss, D. Constantinescu, G. Steinbrecher, M. Vlad, F. Spineanu, et al., Noble internal transport barriers and radial subdiffusion of toroidal magnetic lines, Ann. Phys. 28 (6) (2003) 87.

[25] A.B. Schelin, K.H. Spatschek, Directed chaotic transport in the tokamap with mixed phase space, Phys. Rev. E 81 (2010) 016205.

[26] R. Wittkowski, A.B. Schelin, K.H. Spatschek, Mean motion in stochastic plasmas with a space-dependent diffusion coefficient, Contrib. Plasma Phys. 49 (2009) 55.